HHS Public Access

Author manuscript

Nat Immunol. Author manuscript; available in PMC 2019 June 03.

Published in final edited form as:

Nat Immunol. 2019 January ; 20(1): 97–108. doi:10.1038/s41590-018-0260-6.

The establishment of resident memory B cells in the lung requires local antigen encounter

S. Rameeza Allie[1], **John E. Bradley**[1], **Uma Mudunuru**[1], **Michael D. Schultz**[2], **Beth A. Graf**[2], **Frances E Lund**[2], and **Troy D. Randall**[1,*]

[1]Department of Medicine, Division of Clinical Immunology and Rheumatology, University of Alabama at Birmingham, Birmingham, AL 35294

[2]Department of Microbiology, University of Alabama at Birmingham, Birmingham, AL 35294

Abstract

Memory B cells are found in lymphoid and non–lymphoid tissues, suggesting that some may be tissue–resident cells. Here we show that pulmonary influenza infection elicited lung–resident memory B cells (BRM cells) that were phenotypically and functionally distinct from their systemic counterparts. BRM cells were established in the lung early after infection, in part because their placement required local antigen encounter. Lung BRM cells, but not systemic memory B cells, contributed to early plasmablast responses following challenge infection. Following secondary infection, antigen–specific BRM cells differentiated *in situ*, whereas antigen–non–specific BRM cells were maintained as memory cells. These data demonstrate that BRM cells are an important component of immunity to respiratory viruses like influenza and suggest that vaccines designed to elicit BRM cells must deliver antigen to the lung.

Introduction

Durable humoral immunity is maintained by long–lived, antibody–secreting plasma cells that home to the bone marrow[1, 2], as well as resting memory B cells that are poised to respond rapidly following a secondary encounter with antigen[3]. The generation of both cell types requires help from T cells, typically in the germinal center (GC), where B cells rapidly proliferate and are selected for high–affinity antigen receptors[4, 5]. As GC B cells differentiate into memory cells, they stop proliferating[6, 7], and in some cases, home to

*Correspondence to: Troy Randall, Department of Medicine, Division of Clinical Immunology and Rheumatology, 1720 2nd AVE S. SHEL 507, University of Alabama at Birmingham, Birmingham, AL 35294, Phone: 205–975–33123, Fax: 205–975–3322, randallt@uab.edu.

Author contribution.

S.R.A., F.E.L. and T.D.R. designed the experiments. J.E.B., B.A.G. and T.D.R. designed the recombinant influenza proteins and J.E.B. and B.A.G. expressed, purified and characterized the tetramers. U.M. and S.R.A performed the surgeries. M.D.S. performed the intratracheal infections. S.R.A performed and analyzed the experiments and generated the figures. S.R.A. and T.D.R. wrote the manuscript. All authors edited the manuscript.

Data Availability.

The data supporting the findings of this study are available from the corresponding authors upon request.

Competing interests statement.

The authors do not have any competing financial or non-financial interests as defined by Nature Research.

mucosal surfaces[8, 9]. For example, pulmonary infection with influenza virus elicits memory B cells in the lung that express CXCR3[9], whereas memory B cells responding to intestinal infection with rotavirus express mucosal homing receptors, such as $\alpha_4\beta_7$ integrin and CCR9[8].

Early studies of memory B cells in the lung use limiting dilution and *in vitro* differentiation to indirectly enumerate memory B cells by ELISPOT[10], but do not directly characterize the memory B cells themselves. More recent studies use fluorescently labeled hemagglutinin (HA) to identify influenza–specific B cells in the lung and show that these cells have hallmarks of resident memory cells, such as the expression of CD69[9]. Importantly, following adoptive transfer, memory B cells from the lung respond more quickly to challenge infection than those from lymphoid organs[9], suggesting that memory B cells in different locations may be functionally distinct.

Although these studies imply that resident memory B (BRM) cells are generated following influenza infection, they do not test whether potential BRM cells in the lung recirculate or whether they alter the properties of a secondary B cell response following infection. In fact, it is not clear whether BRM cells in the lung would benefit pulmonary immunity. For example, lung–resident memory T (TRM) cells, are a critical element of pulmonary immunity because they must physically contact MHC–expressing target cells in a secondary response in order to exert their effector functions[11]. In contrast, memory B cells either differentiate into antibody–secreting cells (ASCs) or re–enter the GC and undergo additional rounds of proliferation and selection[12, 13]. Both of these functions can be efficiently accomplished in draining lymph nodes. Given that antibodies generated in the lymph node circulate systemically and efficiently protect the lung[14], it is not clear whether BRM cells might be useful or even if they exist at all.

Here we used parabiosis to definitively demonstrate the presence of BRM cells in the lung following influenza infection. We found that influenza–specific BRM cells, particularly IgM$^+$ BRM cells, were established early after influenza infection and were phenotypically distinct from their lymphoid counterparts. The formation of BRM cells that colonize the lung was dependent on early CD40–dependent interactions with T cells in lymphoid organs. However, the placement of BRM cells in the lung also required encounter with antigen in the lung itself. Importantly, the presence of BRM cells in the lung led to a rapid secondary ASC response in the lung following a challenge infection. This rapid secondary response was maintained when mice were treated with the S1P1R agonist FTY–720 to prevent lymphocyte recirculation, suggesting that BRM cells differentiated *in situ* rather than in draining lymph nodes. Taken together, these data suggest that, along with resident memory T cells, BRM cells in the lung contribute to protection against secondary pulmonary infections.

Results

Identification of influenza–specific B cells

In order to identify influenza–specific B cells, we expressed recombinant nucleoprotein (NP) monomers with a biotinylation domain and a 6×his tag in *Escherichia coli* and expressed recombinant hemagglutinin (HA) from the A/PR8/34 (PR8 – H1N1) and A/X31 (X31 –

H3N2) viruses with a GNC4 trimerization domain and either a 6×his tag or a biotinylation (Avi) domain in 293 cells (Fig. 1a). Following purification over a nickel column (Fig. 1b), we enzymatically biotinylated the purified recombinant HA proteins, and "tetramerized" the recombinant HA and NP proteins with fluorochrome–conjugated streptavidin to generate reagents that could be used in flow cytometry assays.

To determine whether our B cell tetramers could identify antigen–specific cells, we infected C57BL/6 mice with either PR8 or with X31 and determined the frequency of tetramer–binding cells in the GC population (complete gating strategy in Supplementary Fig. 1) from the mediastinal lymph node (mLN). In mice infected with PR8 for 15 days, we found that about 10% of the GC B cells bound the HA(PR8) tetramer and 40% bound the NP tetramer, but very few B cells bound the HA(X31) tetramer (Fig. 1c). Conversely, in mice infected with X31, about 4% of the GC B cells bound the HA(X31) tetramer and about 43% bound the NP tetramer, but very few bound the HA(PR8) tetramer (Fig. 1d). We also observed both NP–specific and HA(PR8)–specific cells in the $CD138^{+}$ plasmablast population and in the $CD38^{+}IgD^{-}PNA^{-}$ memory B cell population in the mLNs of PR8–infected mice (Fig. 1e,f).

To further confirm that we were identifying antigen–specific memory B cells rather than non–specific binding to sialic acid (for HA tetramers), we next gated on isotype–switched memory B cells in the mLNs of naïve, PR8–infected and *Schistosoma mansoni*–infected mice (Fig. 1g–i). We found essentially no binding of either the NP or HA(PR8) tetramers to isotype–switched memory B cells in either the naïve or *S. mansoni*–infected mice, but observed about 11% NP–specific and 5% HA(PR8)–specific isotype–switched memory B cells in PR8–infected mice (Fig. 1h). Both IgM^{+} memory B cells and isotype–switched memory B cells could be found in lungs, spleen and mLNs of PR8–infected mice, but not in naïve mice on day 30 and day 70 after infection (Supplementary Fig. 2). These results demonstrate the specificity of the B cell tetramer reagents.

BRM cells in the lung and lymphoid tissues are distinct

To characterize non–circulating memory B cells in the mLN, lung and spleen, we infected mice with PR8 and 56 days later, infused them with fluorochrome–conjugated anti–B220, 5 min prior to euthanasia. We subsequently gated on $CD19^{+}B220^{-}$ (non–circulating) $CD38^{hi}$ isotype–switched memory B cells and finally gated on NP–binding cells (Fig. 2a–d). We found that the majority of NP–specific isotype–switched memory B cells in the mLN and spleen expressed CD73 (Fig. 2e), a marker noted in previous memory B cell studies[15], whereas most isotype–switched memory B cells in the lung did not express CD73. NP–specific memory B cells in the lung also differed from those in the mLN and spleen based on the expression of CD80 and PD–L2 (Fig. 2f).

Resident memory T cells in the lung are often characterized using CD69 and CD103[11]. Although most NP–specific memory B cells in all three tissues expressed CD69, none of them expressed CD103 (Fig. 2g). Moreover, although approximately 12% of the BRM in mLN and spleen expressed the LN homing receptor, CD62L, almost none of the BRM cells in the lung expressed this marker (Fig. 2h). Finally, NP–specific memory B cells in the lung uniformly expressed high amounts of CXCR3, whereas those in the mLN and spleen had a substantial population of $CXCR3^{-}$ cells (Fig. 2i). These characteristics were generally

shared between NP–specific isotype–switched memory B cells in the non–circulating ($B220^{-}$) and total ($B220^{+/-}$) populations (Supplementary Fig. 3a–b), although we should note that more than 95% of NP–specific isotype–switched memory B cells in the lung and mLN are in the $B220^{-}$ fraction. Despite the phenotypic differences between memory B cells in the lungs and lymphoid organs, the distribution of isotypes was remarkably similar, except for an increase in the frequency of IgM^{+} BRM cells in the spleen (Fig. 2j and Supplementary Fig. 3c–e). These results demonstrate that BRM cells in the lung are phenotypically different from their lymphoid counterparts.

BRM cells in the lung do not recirculate

To determine whether the non–circulating, influenza–specific memory B cells permanently resided in the lung, we infected C57BL/6 (CD45.2) mice with influenza and on day 44, surgically paired them with CD45.1 partner mice for an additional 15 days to allow recirculating cells to equilibrate between the partners. To determine whether the pairs had reached equilibrium, we enumerated both donor ($CD45.2^{+}$) and partner ($CD45.2^{-}$) naïve B cells in the mLN and spleen. We found that naïve B cells had equilibrated between donor and partner mice in the mLNs and spleens of both mice in each pair (Fig. 3a,b).

We next gated on non–circulating IgM^{+} or isotype–switched memory B cells in the lung and examined whether the NP–specific memory B cells had equilibrated (Fig. 3c). When PR8–memory mice were paired with naïve mice, NP–specific IgM^{+} memory B cells as well as NP–specific isotype–switched memory B cells remained in the previously infected lung and did not migrate to the naïve lung (Fig. 3d,e). We also paired previously infected CD45.2 mice with CD45.1 mice that had previously received intranasal lipopolysaccharide (LPS) to promote pulmonary inflammation. Again, we found that NP–specific IgM^{+} memory B cells as well as NP–specific, isotype–switched memory B cells remained in the previously infected lung and did not migrate to the LPS–treated lung (Fig. 3f,g). Finally, we paired previously infected CD45.2 mice with previously–infected CD45.1 mice so that both lungs had been exposed to virus. Again, we found that NP–specific IgM^{+} memory B cells as well as NP–specific, isotype–switched memory B cells remained in the lung of origin and did not migrate to the opposite lung (Fig. 3h,i). These data suggest that antigen specific memory cells in the lung are maintained as tissue resident cells (BRM cells) and do not migrate, even to previously infected lungs.

We also tested whether tissue–residence was restricted to the lung or also occurred in the mLN and spleen. Using PR8–infected CD45.1 mice paired with PR8–infected CD45.2 mice, we found that both HA–specific and NP–specific memory B cells in both the IgM^{+} and isotype-switched fractions were strongly biased to remain in the lung of origin (Supplementary Fig. 4a–d). This bias was less pronounced in the mLN and was only significant in the isotype–switched memory B cells (Supplementary Fig. 4e–h). The bias was even less evident in the spleen, but did achieve significance for NP–specific IgM^{+} and isotype–switched memory B cells (Supplementary Fig. 4i–l).

Memory B cells are established early after immunization[7]. To determine whether BRM cells in the lung are also established early after infection, we infected both CD45.1 and CD45.2 mice with PR8, surgically paired them 15 days later and evaluated the presence of BRM

cells 15 days after joining. We found that naïve B cells in mLN and spleen had equilibrated in the parabiotic pairs (Fig. 4a,b). However, after gating on non–circulating memory B cells (Fig. 4c), we found that NP–specific IgM^+ memory B cells as well as NP–specific isotype–switched memory B cells primarily remained in the partner of origin (Fig. 4d,e). HA–specific IgM^+ memory B cells as well as HA–specific, isotype–switched memory B cells also primarily remained in the partner of origin (Fig. 4f,g). Collectively, these findings demonstrate that many BRM cells in the lung are established very early after infection.

BRM cells are formed by early CD40–dependent mechanisms

To establish the kinetics of GC formation relative to BRM generation, we enumerated antigen–specific GC B cells in the mLN, as well as isotype–switched memory B cells in the blood and lung. We found that GC B cells appeared in the mLN as early as 7 days after infection, peaked around 15 days after infection and declined thereafter (Fig. 5a). In contrast, memory B cells in both the blood (Fig. 5b) and lung (Fig. 5c) were barely detectable at day 7, but peaked at day 15 and declined thereafter.

To test whether the appearance of BRM in the lung was dependent on CD40 signaling, we infected mice with PR8 and treated them at various intervals with a blocking antibody against CD40L (MR1). We found that CD40L blockade for 2 weeks (regardless of when the treatment started) completely eliminated the GC B cell response in both the mLN and in the lung (Fig. 5d–g). Early CD40L blockade prevented the placement of NP–specific IgM^+ and isotype–switched BRM cells in the lung (Fig. 5h). Reductions in BRM cells were less pronounced when the blockade occurred between days 10 and 20 (Fig. 5i) or between days 20 and 30 (Fig. 5j). However, BRM cells in the lung were not reduced when CD40L was blocked between days 30–40 (Fig. 5k), despite a complete loss of GC B cells in the mLN and lung. We obtained a similar result when we examined HA–specific BRM cells (Supplementary Fig. 5), although the IgM^+ BRM cells were placed in the lung as early as day 10, whereas the isotype–switched memory B cells required up to 30 days to fill the lung compartment. These data indicated that the seeding of influenza–specific BRM cells in the lung is dependent on early T cell interactions, possibly in the GC, and that IgM^+ BRM cells are seeded earlier than isotype–switched BRM cells.

BRM establishment in the lung is dependent on local antigen

To test whether local antigen was needed for the placement of BRM in the lung, we surgically paired naïve mice, waited 15 days for them to attain equilibrium, infected one mouse with PR8 and the other with X31 and analyzed the influenza–specific BRM cells in the lungs 10 days later. After gating on non–circulating isotype–switched memory B cells (Fig. 6a), we found that PR8–infected partners had many more HA(PR8)–specific BRM cells than the X31–infected partners (Fig. 6b). Conversely, we found that the X31–infected partners had many more HA(X31)–specific BRM cells than the PR8–infected partners (Fig. 6b). Importantly, both partners had similar numbers of NP–specific BRM cells (Fig. 6b). These data demonstrate that even in concurrently infected partner mice, BRM cells tend to stay in the lungs that express the antigen to which they respond.

We next tested whether antigen–non–specific pulmonary inflammation could recruit pre–existing systemic memory B cells to the lung. To do this, we infected mice with PR8 in the peritoneal cavity (or not), challenged them (or not) 30 days later with X31 and examined the placement of NP–specific, HA(X31)–specific and HA(PR8)–specific memory B cells (Fig. 6c). We found that peritoneal infection with PR8 did not elicit either NP–specific (Fig. 6d) or HA(PR8)–specific (Fig. 6e) isotype–switched memory B cells in the lung. As expected, a pulmonary challenge with X31 elicited both NP–specific (Fig. 6d) and HA(X31)–specific (Fig. 6f) isotype–switched memory B cells in the lung. Importantly, pulmonary challenge with X31 also recruited HA(PR8)–specific isotype–switched memory B cells to the lung (Fig. 6e). We observed similar results on day 10 (Fig. 6d–f) and day 45 (Fig. 6g–i) after the challenge infection. We also examined IgM^+ memory B cells in the same experiment, but found that so few HA(PR8)–specific IgM^+ memory B cells were recruited to the lungs that the result was not significant (Supplementary Fig. 6c, f). Taken together, these data indicate that BRM cells need to encounter antigen again for their placement in the lung.

BRM cells in the lung respond rapidly to infection

To directly compare the ability of systemic or pulmonary infection to elicit BRM cells in the lung, we infected mice in either the peritoneal cavity or the lung (or mock infected) and after 30 days enumerated NP–specific B cell**s.** As expected, naïve mice lacked NP–specific GC B cells (Fig. 7a) or isotype–switched memory B cells (Fig. 7b), whereas the spleens of mice infected in the peritoneal cavity or the lung had numerous NP–specific GC and isotype–switched memory B cells. In contrast, only the lungs of mice intranasally infected with PR8 had NP–specific isotype–switched memory B cells (Fig. 7c). To test the effect of lung BRM cells on the outcome of a challenge infection, we intraperitoneally, intranasally or mock infected mice with PR8, challenged all groups with X31 on day 30 and measured weight loss over 2 weeks and assayed viral titers on day 35. We found that intranasally primed mice had the smallest drop in weight (Fig. 7d) and the lowest viral titers (Fig. 7e).

Although intranasally infected mice have BRM cells, they also likely have resident memory T cells, which undoubtedly contribute to secondary immunity. To test whether BRM cells participate in pulmonary recall responses, we enumerated antibody–secreting cells (ASCs) by ELISPOT in mice that were intraperitoneally, intranasally or mock infected for 30 days, and subsequently challenged with X31 (or not) for 4 days. We found that naïve and peritoneally infected mice completely lacked NP–specific ASCs in their lungs before and after challenge, whereas intranasally infected mice had some NP–specific ASCs in the lung prior to challenge and significantly more ASCs 4 days later (Fig. 8a).

We performed a similar experiment in which BLIMP–1–YFP reporter mice were intraperitoneally, intranasally or mock infected for 30 days, and subsequently challenged with X31 (or not) for 3 days. Given that ASCs strongly express BLIMP-1, we gated on the reporter, YFP, to enumerate ASCs in the lung. We found that naïve and peritoneally infected mice completely lacked NP–specific ASCs in their lungs before and after challenge, whereas intranasally infected mice had some NP–specific ASCs in the lung prior to challenge and significantly more ASCs 3 days later (Fig. 8b). To test whether the ASCs remaining in the lung following a primary infection declined over time, we performed the same experiment,

but challenged with X31 at day 60. We found a few remaining ASCs in the lungs of previously–infected mice, but a large increase in the pulmonary ASC response in mice with lung BRM cells, but not in mice with systemic memory B cells (Fig. 8c).

To ensure that the ASCs that we observed in the lungs of challenged mice were due to responding BRM cells and not recirculating memory B cells, we treated PR8 memory mice with FTY720 to block lymphocyte recirculation just before and after challenge with X31. We found that FTY720 did not reduce the NP–specific ASC response in the lung (Fig. 8d), demonstrating that the observed spots were derived from BRM cells that differentiated in situ. We also examined the fate of the BRM cells that reacted with the challenge virus (NP–specific) and the BRM cells that did not react with the challenge virus (HA–PR8–specific). We found that the NP–specific BRM cells declined after challenge (Fig. 8e), whereas the HA(PR8)–specific BRM cells did not (Fig. 8f). Collectively, those findings demonstrate that BRM cells in the lung are important for rapid secondary ASC responses and that inflammatory signals alone are insufficient to trigger the differentiation of BRM cells in the lung[16, 17].

Discussion

Our data show that pulmonary infection with influenza virus elicits non–recirculating, lung–resident BRM cells. Unlike memory B cells in lymphoid organs, BRM cells in the lung uniformly express the chemokine receptor, CXCR3, and completely lack the lymph node homing receptor, CD62L. Moreover, lung–resident BRM cells are evenly divided into $CD73^+$ and $CD73^-$ populations, whereas memory B cells in lymphoid organs are predominantly $CD73^+$. Influenza–specific BRM cells are primarily recruited to the lung in the first few weeks after infection, in part due to local antigen encounter. Finally, the presence of BRM cells in the lung leads to an accelerated ASC response in the lung following a challenge infection. These data demonstrate that, like TRM cells, BRM cells are an instrumental component of pulmonary immunity to influenza.

The formation of BRM cells, like other memory B cells, is dependent on CD40 signaling, most likely in GCs. Interestingly, GCs are found in both the mLN and the lungs of influenza infected mice and some studies suggest that GCs in the lung primarily select for influenza–specific memory B cells in the lung [18]. However, we find that the GC response in the mLN develops very rapidly after infection, whereas the GC response in the lung develops more slowly, likely because it takes time to form inducible bronchus–associated lymphoid tissue (iBALT)[19, 20]. Given our observation that BRM cells in the lung are placed very early after infection and that CD40L blockade at late times has a minimal effect on lung–resident BRM cells, despite eliminating GCs in both the mLN and lung, it seems likely that most lung–resident BRM cells formed in response to a primary infection come from GCs in the mLN.

Interestingly, not all memory B cells transit through GCs, as mice lacking T follicular helper cells, and therefore GCs, still generate memory B cells[21]. Moreover, GC–independent memory B cells poorly express CD73[21]. Given our observation that more than half of the BRM cells in the lung lack CD73, it is possible that some of these cells were generated independently of the GC reaction either in the mLN or in the lung. These data are also

consistent with our observation that many BRM cells, particularly IgM^+ BRM cells, seed the lung very early after infection and with previous studies showing that systemic memory B cells are also primarily formed early after immunization[7].

Although memory B cells are primarily generated early after infection, we still observe them in the blood as late as 70 days after infection, suggesting that recirculating memory B cells could be recruited to the lungs for extended periods of time. In fact, we find that memory B cells established at systemic sites during a primary response can be called into the lung by a subsequent inflammatory response in the lung, such as a non–specific infection. However, during a primary response, the placement of newly–generated BRM precursors in the lung appears to be restricted to a limited time after infection. Moreover, as shown by our experiments with parabiotic mice concurrently infected with two different viruses, the ability to seed the lung is not dictated exclusively by inflammation, which is present in the lungs of both partners, but by the availability of local antigen, suggesting that BRM precursors need to contact antigen in the lung in order to stay (or survive) as lung–resident BRM cells. These data are similar to those showing that the placement of TRM cells in the skin and the lung require contact with local antigen[22, 23].

Where might this encounter with antigen occur? One possibility is that BRM precursors encounter antigen in iBALT[19, 20]. We know that iBALT is formed in the lungs of influenza–infected mice and that mice lacking conventional secondary lymphoid organs generate and maintain long–lived B cell responses[24]. Moreover, GC–like B cells are observed in the lungs of infected mice[19], even though the existence of pulmonary follicular T cells remains controversial[25], possibly due to the altered phenotype of helper T cells in peripheral non–lymphoid tissues[26]. Interestingly, GCs in the lung appear to preferentially select for broadly reactive memory B cells[18], although it is unclear whether the broad reactivity of BRM cells is due to site–specific properties of the GC response or to the early placement of less stringently selected (and perhaps more broadly reactive) BRM cells. This latter idea is consistent with data showing that rapamycin treatment of influenza–infected mice leads to curtailed GC responses, but a more broadly reactive repertoire of memory B cells[27].

Our data highlight another qualitative difference between BRM cells in the lung and memory B cells in lymphoid organs – the rapidity of secondary responses. Mice with NP–specific BRM cells in the lung generate secondary ASC responses in the lungs more rapidly than mice with memory B cells at systemic sites. Importantly, the accelerated secondary response in the lungs is maintained in the presence of FTY–720, a functional antagonist of the chemotactic molecule S1P1[28], demonstrating that the response is generated in situ from precursors already in the lung. This change in secondary response time may be simply due to location, with BRM cells in the lung encountering antigen and inflammation earlier than their lymphoid counterparts and accelerating their response accordingly. Alternatively, BRM cells may be qualitatively different than those in lymphoid organs, as their phenotype suggests, and may be poised to rapidly differentiate into ASCs with minimal stimulation. Consistent with this idea, memory B cells from the lung (presumably BRM cells), adoptively transferred to recipient mice, provide more efficient protection than memory B cells isolated from secondary lymphoid organs[9].

In summary, our data demonstrate that influenza–specific BRM cells are formed in the lung following pulmonary influenza infection and that these cells are necessary for an accelerated ASC response following challenge infection. BRM cells are formed early after infection and seed the lung in a process that depends on local encounter with antigen. These data suggest that vaccines designed to elicit highly effective, long–lived protection against influenza virus infection will need to deliver antigens to the respiratory tract.

METHODS

Mice and parabiosis.

Male and female C57BL/6J (CD45.2) and B6.SJL–*Ptprc*^{a}*Pepc*^{b}/BoyJ (CD45.1) mice were purchased from the Jackson Laboratory and BLIMP–1–YFP reporter mice[29] were obtained from S. Crotty (La Jolla Institute for Immunology) and bred in the University of Alabama at Birmingham vivarium as noted in the Life Sciences Reporting Summary associated with this paper. Swiss Webster mice infected with *Schistosoma mansoni* (strain NMRI) were obtained from the Schistosomaisis Resource Center and distributed through BEI resources, National Institute of Allergy and Infectious Diseases. Parabiosis surgery was performed as described[24], using pairs of female mice that had been co–housed for at least 2 weeks prior to surgery. In brief, anesthetized mice were shaved and disinfected with betadine and longitudinal incisions in the skin were made from approximately 1 cm behind the ear to just past the hind limb without opening the peritoneal cavity. The skin was loosened from the connective tissue and the two mice were sutured together at the scapulae, flank and thigh. The dorsal edges of the skin were joined using 9 mm stainless steel wound clips. Body temperature was maintained using a heating pad during surgery and recovery. Mice were provided buprenorphine (0.05 mg/kg) prior to surgery and carprofen (5 mg/kg) prior to surgery and 24 h post–surgery. All animal procedures were approved by the University of Alabama Institutional Animal Care and Use Committee and were performed according to guidelines outlined by the National Research Council.

Infections and viral foci assay.

Influenza A/PR8/34 (PR8) was used at 15,000 viral foci units (VFU) for intranasal infection and at 1×10^9 VFU for intraperitoneal infection. In Figure 7a–d, the i.p. infections were repeated for 6 days at 1×10^8 VFU, 1×10^8 VFU, 1×10^9 VFU, 1×10^9 VFU, 1×10^8 VFU and 1×10^8 VFU. Influenza X31 was used at 1.25×10^4 VFU for primary infection and 1.25×10^5 VFU for secondary infections. Mice were anesthetized with vaporized isofluorane and infected intranasally with 100 μl of inoculum or intratracheally with 75 μl inoculum. Viral foci assays were performed by homogenizing lung samples in zero–serum medium with 4 μg/ml trypsin and performing 5–fold serial dilutions in the same media. 100 μl of each sample was used to infect MDCK cell monolayers. After 16 h of culture, MDCK cells were fixed with 80% acetone and infected cells were detected using an antibody against NP (Clone A3. Millipore–Sigma). Spots were revealed using alkaline phosphatase–conjugated streptavidin (Life Technologies) and BCIP/NBT substrate (Moss Substrates Inc.). Samples were plated in duplicates and the mean foci count was used to calculate the VFU per ml of sample.

Antibody infusion, blocking antibodies and FTY–720 treatment.

To identify circulating B cells, mice were intravenously administered 2.4 μg of fluorochrome–conjugated anti–B220 in 100 μl PBS, 5 min prior to euthanasia. CD40:CD40L interactions were blocked with 250 μg of MR1 (BioXCell). To prevent lymphocyte recirculation, the S1P1R agonist, FTY–720, was dissolved at 10 mg/ml in DMSO, diluted to 0.5 mg/ml in ethanol and mixed 50:50 with PBS prior to administration at 1 mg/kg.

Tissue preparation and flow cytometry.

Lungs were isolated, cut into small fragments and digested for 30 min at 37 °C with 0.6 mg/ml collagenase A (Sigma) and 30 μg/ml DNAse I (Sigma) in RPMI–1640 medium (GIBCO). Digested lungs, mLNs or spleens were mechanically disrupted by passage through a wire mesh. Red blood cells were lysed with 150 mM NH_4Cl, 10 mM $KHCO_3$ and 0.1 mM EDTA. Fc receptors were blocked with 5 μg/ml anti–CD16/32 (BD–Biosciences), followed by staining with fluorochrome–conjugated antibodies. Analytic flow cytometry was performed on a LSR II (BD–Biosciences) instrument available through the Comprehensive Flow Cytometry Core at UAB.

Production of influenza proteins, immunoblot and tetramers.

The coding sequences of PR8 $HA_{16–523}$ (accession number: P03452) and X31 $HA_{15–525}$ (accession number: P03438) were synthesized in frame with the human CD5 signal sequence upstream and the GCN4 isoleucine zipper trimerization domain downstream (GeneArt). These cDNAs were fused in frame with either a 6XHIS tag or an AviTag at the C–terminus and cloned into the pCXpoly(+) mammalian expression vector. Constructs encoding HA–6XHIS and HA–AviTag were co–transfected using 293Fectin Transfection Reagent into FreeStyle™ 293–F Cells (ThermoFisher Scientific) at a 2:1 ratio, respectively. Transfected cells were cultured in FreeStyle 293 Expression Medium for 3 days and the supernatant was recovered by centrifugation. Recombinant HA molecules were purified by FPLC using a HisTrap HP Column (GE Healthcare) and eluted with 250 mM of imidazole. The coding sequence of NP from PR8 was synthesized in frame with the coding sequence for a 15 amino acid biotinylation consensus site[30] on the 3′ end (GeneArt). The modified NP sequence was cloned in frame to the 6X His tag in the pTRC–His2c expression vector (Invitrogen). NP protein was expressed in *E. coli* strain CVB101 (Avidity) and purified by FPLC using a HisTrap HP Column (GE Healthcare) and eluted with with a 50–250 mM gradient of imidazole. Purified HA was biotinylated by addition of biotin–protein ligase (Avidity). Biotinylated proteins were then tetramerized with fluorochrome–labeled streptavidin (Prozyme,). Labeled tetramers were purified by size exclusion on a HiPrep 16/60 Sephacryl S–300 column (GE Healthcare).

ELISPOT.

For ELISPOT assays, multiscreen HA plates (MAHAS4510 – Millipore) were coated with purified NP at 1 μg/ml in PBS overnight at 4 °C. Plates were washed with PBS and blocked with complete media (RPMI supplemented with 10% FBS, 0.5% Penicillin (100×), 0.5% Streptomycin (100×), 1% L–Glutamine (200 mM), 1% sodium pyruvate (100mM), 1%

HEPES pH7.4 (1M), 0.15% sodium bicarbonate, 1.2% amino acids (50×), 1.2% non–essential amino acids (100×), 1.2% vitamins (100×), 0.7% glucose, 0.1% 2–mercaptoethanol (1000×, 55 mM). Single–cell suspensions were washed, diluted in complete media and cultured on coated plates for 5 hours. Cells were aspirated, and plates were washed with 0.2% Tween 20 in PBS. Bound IgG was detected using alkaline phosphatase–conjugated goat anti–mouse Kappa (Southern Biotech) diluted (1:1000) in in 0.5% BSA, 0.05% Tween 20 in PBS for 1 h at 37 °C. Plates were washed with 0.2% Tween 20 in PBS and developed with BCIP/NBT (Moss Substrates Inc.) substrate for 1 hour. Spots were recorded using a CTL Immunospot S6 Macroplate Imager Reader (New Life Scientific Inc.) and counted manually.

Statistical analysis.

GraphPad Prism software (Version 7.0) was used for data analysis. Data sets that did not follow a Gaussian distribution were analyzed using non–parametric tests. Comparisons between two samples were performed with Student's t test or the Mann–Whitney U test. Parabiosis experiments were analyzed using one–way ANOVA (paired) followed by the Bonferroni–Sidak method for multiple comparison. One–way ANOVA, followed by analysis specific post–tests, were carried out when greater than two variables were compared. A P value < 0.05 was considered statistically significant.

Supplementary Material

Refer to Web version on PubMed Central for supplementary material.

Acknowledgements.

The authors would like to thank U. Mudunuru and S. Simpler for animal husbandry and the Rheumatic Diseases Core Center flow cytometry facility that is supported by AI078907. This work was supported by NIH grants HL69409, AI100127, AI097357, AI109962 to T.D.R. and AI120508 to S.R.A.

References.

1. Halliley JL et al. Long-Lived Plasma Cells Are Contained within the CD19^{-}CD38^{hi}CD138^{+} Subset in Human Bone Marrow. Immunity 43, 132–145 (2015). [PubMed: 26187412]
2. Dorner T & Radbruch A Antibodies and B cell memory in viral immunity. Immunity 27, 384–392 (2007). [PubMed: 17892847]
3. Phan TG & Tangye SG Memory B cells: total recall. Curr. Opin. Immunol 45, 132–140 (2017). [PubMed: 28363157]
4. Bannard O & Cyster JG Germinal centers: programmed for affinity maturation and antibody diversification. Curr. Opin. Immunol 45, 21–30 (2017). [PubMed: 28088708]
5. Shlomchik MJ & Weisel F Germinal center selection and the development of memory B and plasma cells. Immunol. Rev 247, 52–63 (2012). [PubMed: 22500831]
6. Schittek B & Rajewsky K Maintenance of B-cell memory by long-lived cells generated from proliferating precursors. Nature 346, 749–751 (1990). [PubMed: 2388695]
7. Weisel FJ, Zuccarino-Catania GV, Chikina M & Shlomchik MJ A Temporal Switch in the Germinal Center Determines Differential Output of Memory B and Plasma Cells. Immunity 44, 116–130 (2016). [PubMed: 26795247]
8. Jaimes MC et al. Maturation and trafficking markers on rotavirus-specific B cells during acute infection and convalescence in children. J. Virol 78, 10967–10976 (2004). [PubMed: 15452217]

9. Onodera T et al. Memory B cells in the lung participate in protective humoral immune responses to pulmonary influenza virus reinfection. Proc. Natl. Acad. Sci. U. S. A 109, 2485–2490 (2012). [PubMed: 22308386]
10. Joo HM, He Y, Sundararajan A, Huan L & Sangster MY Quantitative analysis of influenza virus-specific B cell memory generated by different routes of inactivated virus vaccination. Vaccine 28, 2186–2194 (2010). [PubMed: 20056191]
11. Schenkel JM & Masopust D Tissue-resident memory T cells. Immunity 41, 886–897 (2014). [PubMed: 25526304]
12. Dogan I et al. Multiple layers of B cell memory with different effector functions. Nat. Immunol 10, 1292–1299 (2009). [PubMed: 19855380]
13. Pape KA, Taylor JJ, Maul RW, Gearhart PJ & Jenkins MK Different B cell populations mediate early and late memory during an endogenous immune response. Science 331, 1203–1207 (2011). [PubMed: 21310965]
14. Palladino G, Mozdzanowska K, Washko G & Gerhard W Virus-neutralizing antibodies of immunoglobulin G (IgG) but not of IgM or IgA isotypes can cure influenza virus pneumonia in SCID mice. J. Virol 69, 2075–2081 (1995). [PubMed: 7884853]
15. Tomayko MM, Steinel NC, Anderson SM & Shlomchik MJ Cutting edge: Hierarchy of maturity of murine memory B cell subsets. J. Immunol 185, 7146–7150 (2010). [PubMed: 21078902]
16. Bernasconi NL, Traggiai E & Lanzavecchia A Maintenance of serological memory by polyclonal activation of human memory B cells. Science 298, 2199–2202 (2002). [PubMed: 12481138]
17. Lee FE et al. Circulating human antibody-secreting cells during vaccinations and respiratory viral infections are characterized by high specificity and lack of bystander effect. J. Immunol 186, 5514–5521 (2011). [PubMed: 21441455]
18. Adachi Y et al. Distinct germinal center selection at local sites shapes memory B cell response to viral escape. J. Exp. Med 212, 1709–1723 (2015). [PubMed: 26324444]
19. Moyron-Quiroz JE et al. Role of inducible bronchus associated lymphoid tissue (iBALT) in respiratory immunity. Nat. Med 10, 927–934 (2004). [PubMed: 15311275]
20. Hwang JY, Randall TD & Silva-Sanchez A Inducible Bronchus-Associated Lymphoid Tissue: Taming Inflammation in the Lung. Front. Immunol 7, 258 (2016). [PubMed: 27446088]
21. Taylor JJ, Pape KA & Jenkins MK A germinal center-independent pathway generates unswitched memory B cells early in the primary response. J. Exp. Med 209, 597–606 (2012). [PubMed: 22370719]
22. Zaid A et al. Persistence of skin-resident memory T cells within an epidermal niche. Proc. Natl. Acad. Sci. U. S. A 111, 5307–5312 (2014). [PubMed: 24706879]
23. McMaster SR et al. Pulmonary antigen encounter regulates the establishment of tissue-resident CD8 memory T cells in the lung airways and parenchyma. Mucosal Immunol 11, 1071–1078 (2018). [PubMed: 29453412]
24. Moyron-Quiroz JE et al. Persistence and responsiveness of immunologic memory in the absence of secondary lymphoid organs. Immunity 25, 643–654 (2006). [PubMed: 17045819]
25. Vu Van D et al. Local T/B cooperation in inflamed tissues is supported by T follicular helper-like cells. Nat. Commun 7, 10875 (2016). [PubMed: 26915335]
26. Rao DA et al. Pathologically expanded peripheral T helper cell subset drives B cells in rheumatoid arthritis. Nature 542, 110–114 (2017). [PubMed: 28150777]
27. Keating R et al. The kinase mTOR modulates the antibody response to provide cross-protective immunity to lethal infection with influenza virus. Nat. Immunol 14, 1266–1276 (2013). [PubMed: 24141387]
28. Matloubian M et al. Lymphocyte egress from thymus and peripheral lymphoid organs is dependent on S1P receptor 1. Nature 427, 355–360 (2004). [PubMed: 14737169]
29. Misulovin Z, Yang XW, Yu W, Heintz N & Meffre E A rapid method for targeted modification and screening of recombinant bacterial artificial chromosome. J. Immunol. Methods 257, 99–105 (2001). [PubMed: 11687243]
30. Beckett D, Kovaleva E & Schatz PJ A minimal peptide substrate in biotin holoenzyme synthetase-catalyzed biotinylation. Protein. Sci 8, 921–929 (1999). [PubMed: 10211839]

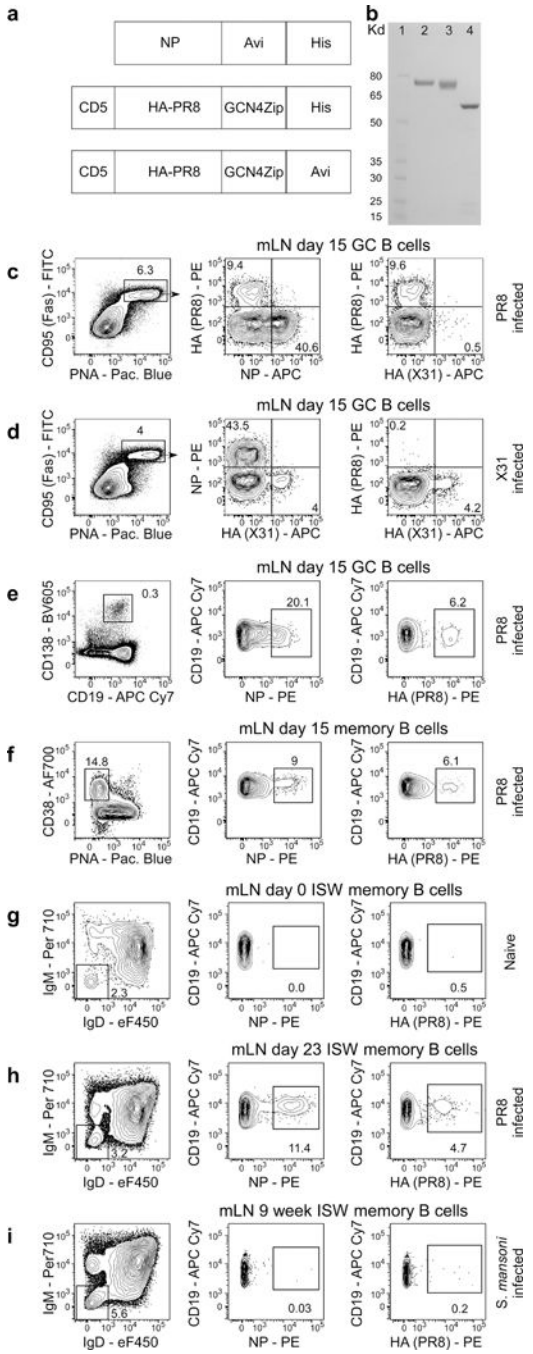

Fig. 1. Identification of influenza–specific B cells.

a. Schematic of recombinant NP and HA proteins. **b**. Coomassie–stained SDS–PAGE gel showing recombinant HA(PR8) (lane 2), HA(X31) (lane 3) and NP (lane 4). Image is representative of 12 independent preparations of recombinant protein. **c–f**. Cells from the mLNs of day 15 influenza–infected mice were first gated on live, singlet, $CD19^+$ lymphocytes (Supplementary Fig. 1a), and then on PNA^+CD95^+ GC B cells (**c–d**), or first gated on live, singlet, lymphocytes (Supplementary Fig. 1a) and then on $CD138^+$ plasmablasts (**e**), or first gated on live, singlet, $CD19^+IgD^-$ lymphocytes (Supplementary

Fig. 1b) and then on $PNA^{lo}CD38^{+}$ memory B cells (**f**). Data are representative of 4 independent experiments with 5 mice. Cells from the mLNs of naïve mice (**g**), day 23 PR8–infected mice (**h**), and week 9 *S. Mansoni*–infected mice (**i**) were gated on live, singlet, $CD19^{+}CD38^{hi}$ lymphocytes (Supplementary Fig. 1c) and analyzed for NP–specific and HA–specific isotype-switched (ISW) memory B cells. Data are representative of 4 experiments with 5 mice.

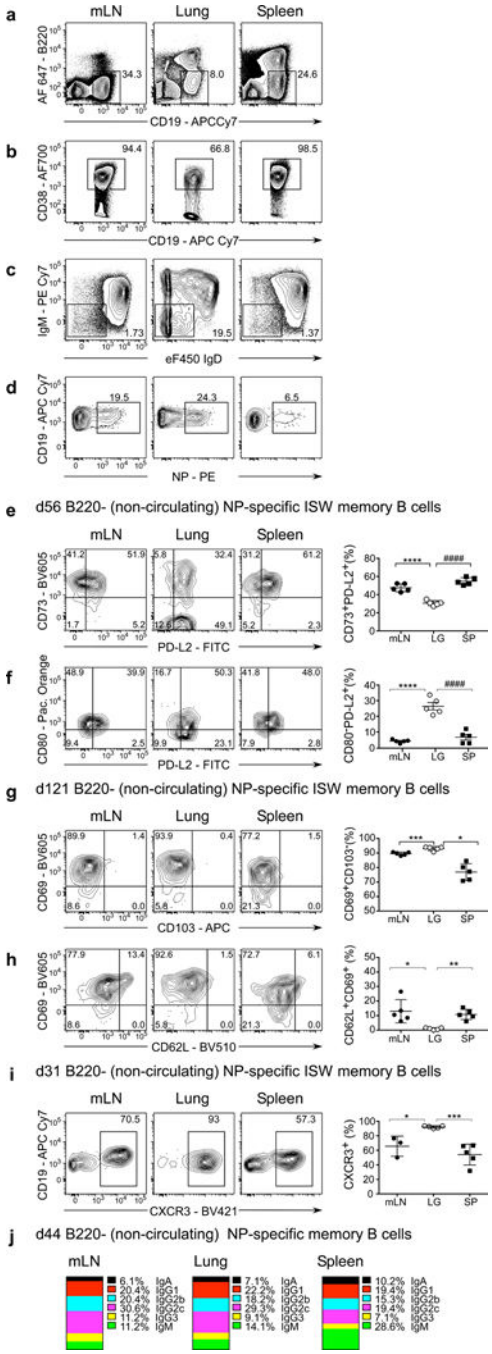

Fig. 2. Phenotype of memory B cells in the lung and lymphoid organs.

PR8–infected mice were infused with anti–B220 5 minutes prior to euthanasia and cells from the mLN, lung and spleen were gated on live, singlet, lymphocytes (Supplementary Fig. 1a) and then on $B220^{-}$ non–circulating B cells (**a**) $CD38^{+}$ memory B cells (**b**), IgD^{-} IgM^{-} ISW cells (**c**) and NP–specific cells (**d**). Within the population of NP–specific memory cells described in panel **d**, we determined the frequencies of $CD73^{+}PD–L2^{+}$ memory B cells (**e**), $CD80^{-}PD–L2^{+}$ memory B cells (**f**), $CD69^{+}CD103^{-}$ memory B cells (**g**), $CD62L^{+}CD69^{+}$ memory B cells (**h**), and $CXCR3^{+}$ memory B cells (**i**). Data are representative of 3

independent experiments with 5 mice (**a–d**), 2 experiments with 5 mice (**g–h**) or 5 experiments with 5 mice. (**i**). Graphs show individual data points as well as mean ± SD. Data were analyzed by one–way ANOVA with Tukey's post–test for multiple comparison, ****p=0.0001 ####p=0.0001 (**e**), ****p=0.0001 ****p=0.0001 (**f**), ***p=0.0002 *p=0.0105 (**g**), *p=0.0471 **p=0.0042 (**h**), *p=0.0206 ***p=0.0008 (**i**). $p<0.05$ is considered significant. Cells from the mLN, lung and spleens of day 44 PR8–infected mice were gated on live, singlet, lymphocytes (Supplementary Fig. 1a), and then gated on NP–specific $CD19^{+}CD38^{+}IgD^{-}$ memory B cells (Supplementary Fig. 3c–e) and the frequency of IgA, IgG1, IgG2b, IgG2c, IgG3 and IgM–expressing cells was determined (**j**). Data are representative of 3 independent experiments with 5 mice.

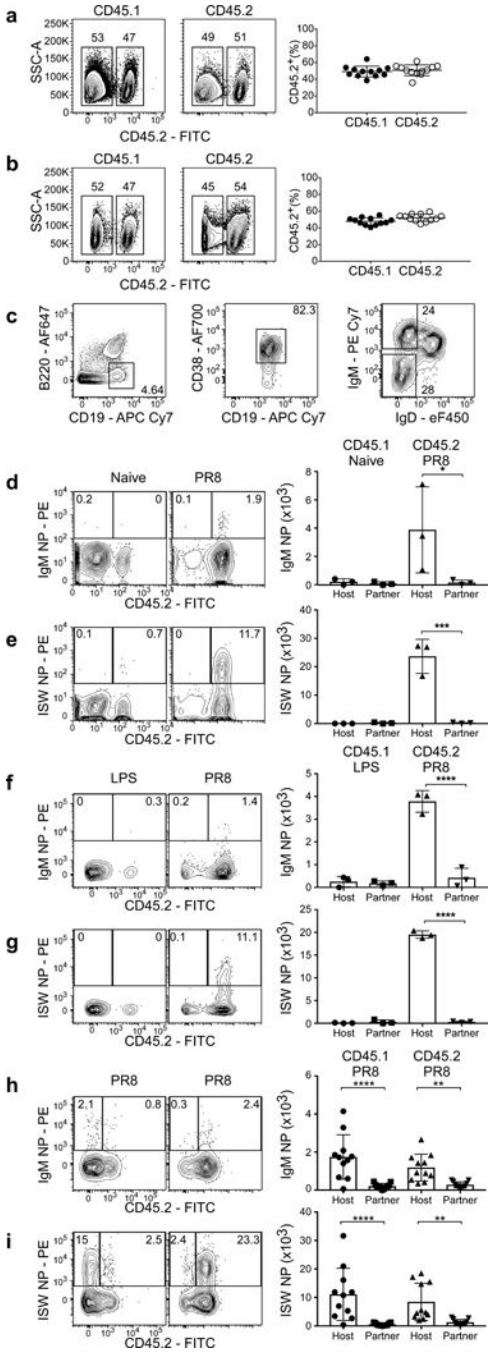

Fig. 3. Identification of influenza–specific, non–circulating BRM cells in the lung.

Mice were infected on day 0, surgically paired with partner mice on day 44 and analyzed on day 59 (**a–i**). Cells from the mLN (**a**) or spleen (**b**) of each partner mouse were gated on live, singlet, lymphocyte $CD19^{+}CD38^{+}IgD^{+}IgM^{lo}$ naïve B cells (Supplementary Fig. 1d) and the frequency of $CD45.2^{+}$ cells was determined in each partner. Data are combined from 4 independent experiments with 3 mice each. Graph shows individual points as well as mean ± SD. Cells from the lung were gated on live, singlet, lymphocytes (Supplementary Fig. 1a) and subsequently gated on $CD19^{+}B220^{-}$ (non–circulating), $CD38^{+}IgD^{-}IgM^{+}$ (IgM) or

$CD38^{+}IgD^{-}IgM^{-}$ (ISW) memory B cells (**c**). The frequencies and numbers of NP–specific IgM (**d**) and ISW (**e**) memory B cells from host and partner mice were determined in the lungs of naïve mice paired with PR8–infected mice. The frequencies and numbers of NP–specific IgM (**f**) and ISW (**g**) memory B cells from host and partner mice were determined in the lungs of LPS–treated mice paired with PR8–infected mice. The frequencies and numbers of NP–specific IgM (**h)** and ISW (**i**) memory B cells from host and partner mice were determined in the lungs of PR8–infected mice paired with PR8–infected mice. Data are representative of 3 independent experiments, each with 3 pairs of mice (**d–e**), 2 experiments with 3 pairs of mice (**f–g**), or 3 experiments combined, totaling 11 pairs of mice (**h–i**). Graphs show individual data as well as mean ± SD. Significance was determined using one–way ANOVA (paired) followed by the Bonferroni–Sidak method for multiple comparison, *p=0.0428 (**d**), ***p=0.0001 (**e–f**), ****p=0.0001, **p=0.0040 (**h**), ****p=0.0001 **p=0.0022 (**i**). $p<0.05$ is considered significant.

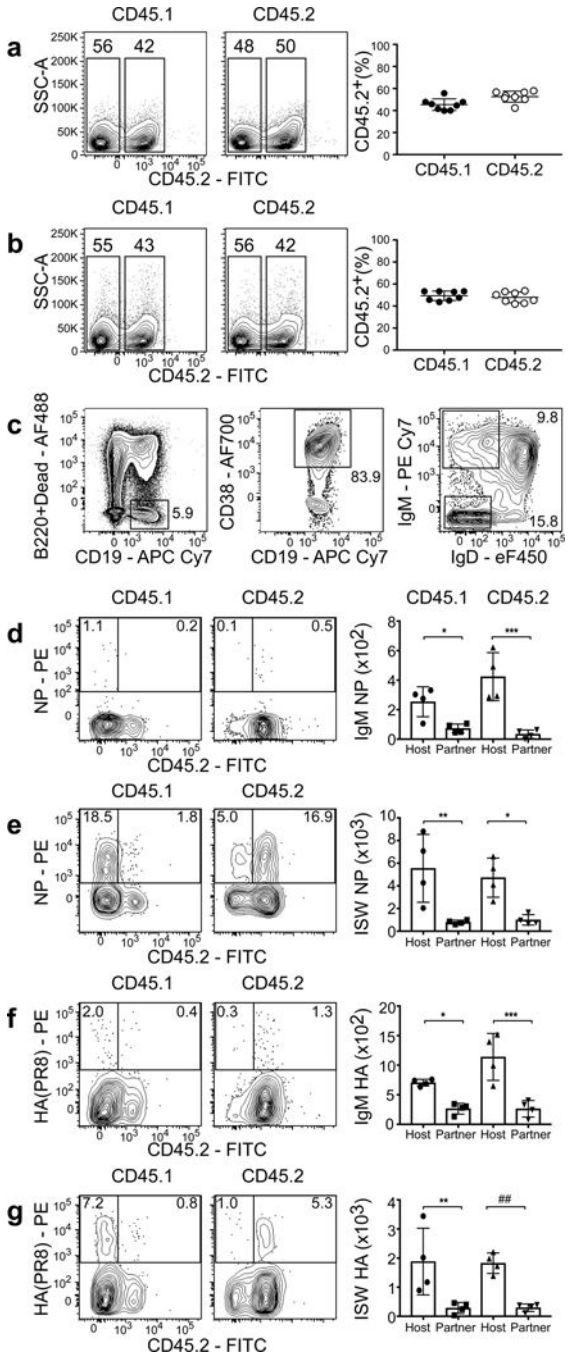

Fig. 4. BRM cells in the lung are established early after infection.

Mice were infected on day 0, surgically paired with partner mice on day 15 and analyzed on day 30 (**a–g**). Cells from the mLN (**a**) or spleen (**b**) were gated on live, singlet, lymphocyte $CD19^{+}IgD^{+}IgM^{lo}$ naïve B cells (Supplementary Fig. 1d) and the frequency of $CD45.2^{+}$ cells was determined in each partner. These data are combined from 2 independent experiments totaling 8 pairs of mice. Graphs show individual data points as well as mean ± SD. Cells from the lung were gated on live, singlets (Supplementary Fig. 1a) and subsequently gated on live, $CD19^{+}B220^{-}$ (non–circulating), $CD38^{+}IgD^{-}IgM^{+}$ (IgM) or $CD38^{+}IgD^{-}IgM^{-}$ (ISW)

memory B cells (**c**). The frequencies of NP–specific IgM (**d**) and ISW (**e**) memory B cells from the lungs of host and partner mice. The frequencies of HA(PR8)–specific IgM (**f**) and ISW (**g**) memory B cells from the lungs of host and partner mice. Data in **c–g** are representative of 3 independent experiments, each with 4 pairs of mice. Graphs show individual data as well as mean ± SD. Significance was determined using one–way ANOVA (paired) followed by the Bonferroni–Sidak method for multiple comparison, *p=0.0457 ***p=0.0002 (**e**), **p=0.0047 *p=0.0213 (**f**), *p=0.0285 ***p=0.0002 (**g**), **p=0.0060 $^{\#\#}$p=0.0080 (**h**). $p<0.05$ is considered significant.

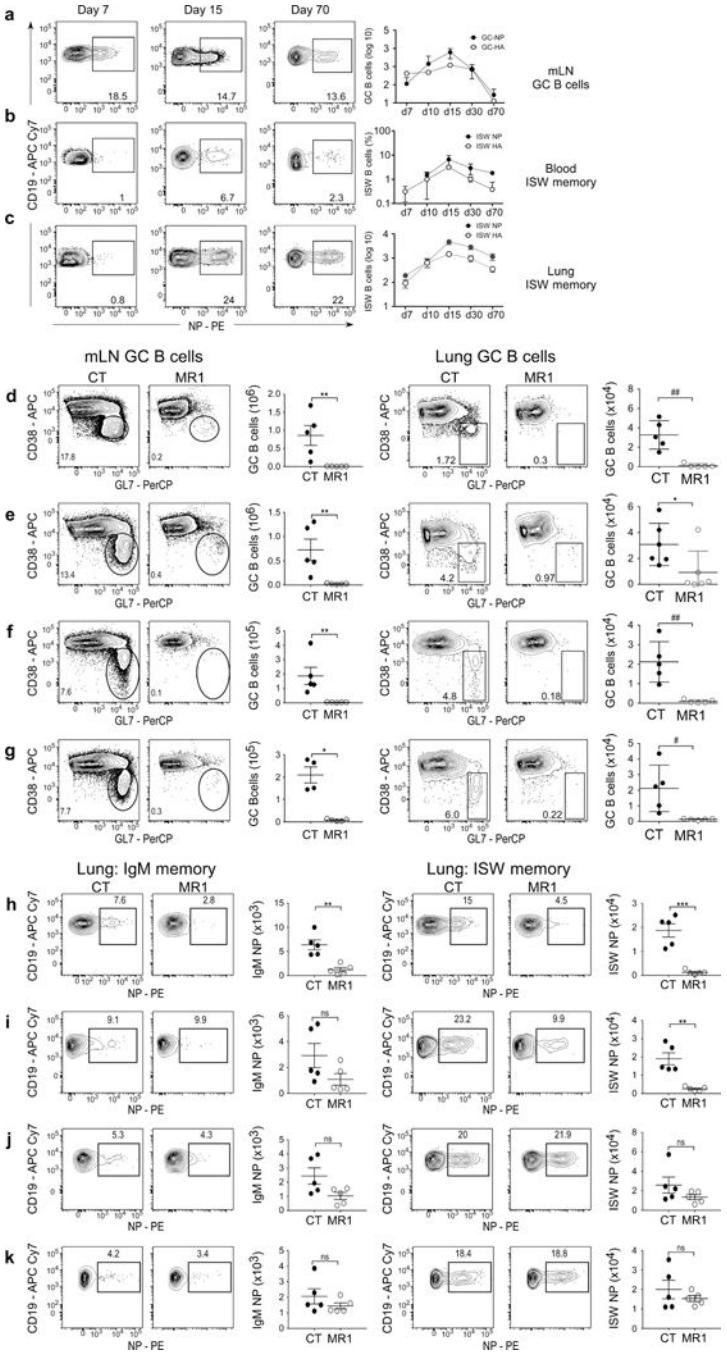

Fig. 5. BRM cells in the lung are generated from early CD40–dependent precursors.

Cells from the mLN of PR8–infected mice were gated on live, singlet, lymphocyte, $CD19^{+}PNA^{+}CD95^{+}$ GC B cells (Supplementary Fig. 1f) and NP–specific as well as HA–specific cells were enumerated (**a**). Cells from the blood (**b**) and lungs (**c**) of PR8–infected mice were gated on live, singlet, lymphocyte, $CD19^{+}CD38^{+}IgM^{-}IgD^{-}$ ISW memory B cells (Supplementary Figure 1c), and the frequency (**b**) and number (**c**) of NP–specific as well as HA–specific cells was determined. Data are representative of 3 independent experiments with 5 mice at each timepoint. The data points represent mean ± SD. Mice were infected

with PR8, administered anti–CD40L (MR1) or isotype control antibody (CT) every other day for 10 days starting on day 5 (**d, h**), day 10 (**e, i**), day 20 (**f, j**) or day 30 (**g, k**). Cells from the mLN and lung were gated on live, singlet, lymphocyte, $CD19^{+}CD138^{lo}$ cells (Supplementary Fig. 1g) and subsequently gated on $GL7^{+}CD38^{lo}$ GC B cells (**d–g**). Cells from the lung were gated on live, singlet, lymphocyte, $CD19^{+}CD138^{lo}CD38^{+}IgM^{+}IgD^{-}$ IgM BRM cells or $CD19^{+}CD138^{lo}CD38^{+}IgM^{-}IgD^{-}$ ISW BRM cells (**h–k**)(gating in Supplementary Fig. 1g). Data in **d–k** are representative of 3 independent experiments with 5 mice/group/timepoint. Graphs show mean ± SD as well as individual data points. Significance was determined using a Mann–Whitney U test, **p=0.0079 $^{\#\#}$p=0.0014 (**d**), **p=0.0079 *p=0.0462 (**e**), **p=0.0079, $^{\#\#}$p=0.0024 (**f**) *p=0.0159 $^{\#}$p=0.0180 (**g**) or unpaired, two–tailed t–test **p=0.0018, ***p=0.0003 (**h**), **p=0.0011 (**i**). $p<0.05$ is considered significant.

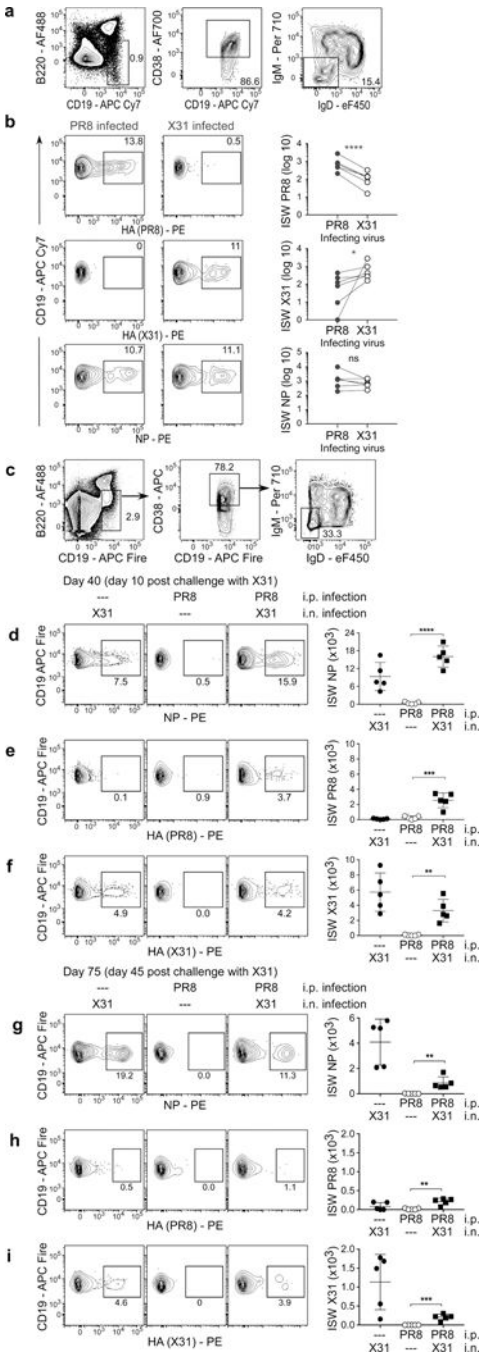

Fig. 6. Establishment of BRM cells in the lung requires local antigen encounter.

Naïve mice were surgically joined and, on day 15, one was infected with PR8 and the other infected with X31 and BRM cells in the lung analyzed on day 25 (**a–b**). Cells from the lung were gated on live, singlet, lymphocytes (Supplementary Fig 1a), and subsequently gated on $B220^{-}CD19^{+}CD38^{hi}IgM^{-}IgD^{-}$ ISW BRM cells (**a**). The frequency and number of HA(PR8)–specific (top row), HA(X31)–specific (middle row) and NP–specific (bottom row) BRM cells were determined in each partner (**b**). Data are representative of 3 independent experiments with 5 pairs of mice. Significance was determined using one–tailed, paired t

test, ****p=0.0001, *p=0.0477. Mice were peritoneally–infected with PR8 on day 0, intranasally challenged with X31 on day 30 and analyzed on days 40 (**d–f**) and day 75 (**g–i**). Cells from the lung were gated on live, singlet, lymphocytes (Supplementary Fig. 1a) and subsequently gated on $CD19^{+}B220^{-}CD38^{+}IgD^{-}IgM^{-}$ ISW memory B cells (**c**). NP–specific (**d,g**), HA(PR8)–specific (**e,h**) and HA(X31)–specific (**f,i**) ISW BRM cells were enumerated on day 40 (**d–f**) and day 75 (**g–i**). These data are representative of 2 independent experiments with 5 mice/timepoint. Data were analyzed with an unpaired t test, ****p=0.0001 (**f**), ***p=0.0009 (**g**), **p=0.0013 (**h**), **p=0.0047 (**i**), **p=0.0011 (**j**), ***p=0.0004 (**k**). $p<0.05$ is considered significant.

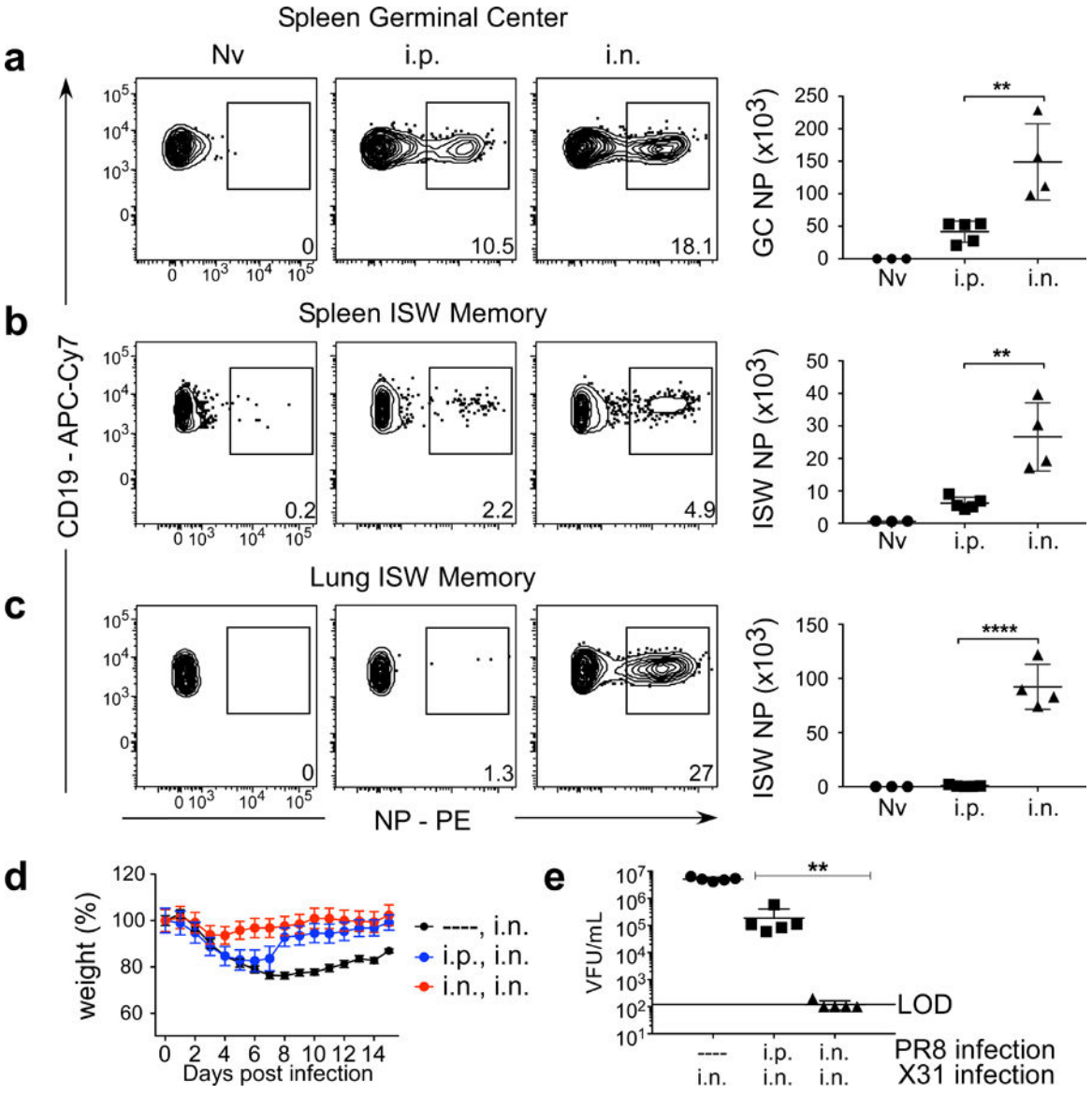

Fig. 7. BRM cells are associated with protection from secondary infection.

Mice were infected in the peritoneal cavity or in the lung and analyzed on day 30 (**a–d**). Cells were gated on live, singlet, lymphocyte, $CD19^{+}B220^{-}CD138^{-}GL7^{+}CD38^{lo}$ GC B cells (Supplemental Fig. 1h) and NP–specific cells were enumerated in the spleen (**a**). Cells were gated on live, singlet, lymphocyte $CD19^{+}B220^{-}CD38^{+}IgD^{-}IgM^{-}$ isotype-switched memory B cells (Supplemental Fig. 1e) and NP–specific cells were enumerated in the spleen (**b**) and lung (**c**). Data are representative of 3 independent experiments with 3 mice in the naïve group, 5 mice in the i.p. infected group and 4 mice in the i.n. infected group. Graphs show mean ± SD as well as individual data points. Significance was determined with a one–way ANOVA with Tukey's post–test for multiple comparisons, **p=0.0038 (**a**), **p=0.0021 (**b**), ****p=0.0001 (**c**). Weight loss after challenge infection (**d**). Viral titers on day 5 after challenge infection (**e**). Data in d, e are representative of 2 experiments with 5 mice/group. Graphs show mean ± SD (d) or individual data points as well as the geometric mean ± SD

(e). Data were analyzed using the Mann–Whitney U test, **p=0.0079. p<0.05 is considered significant.

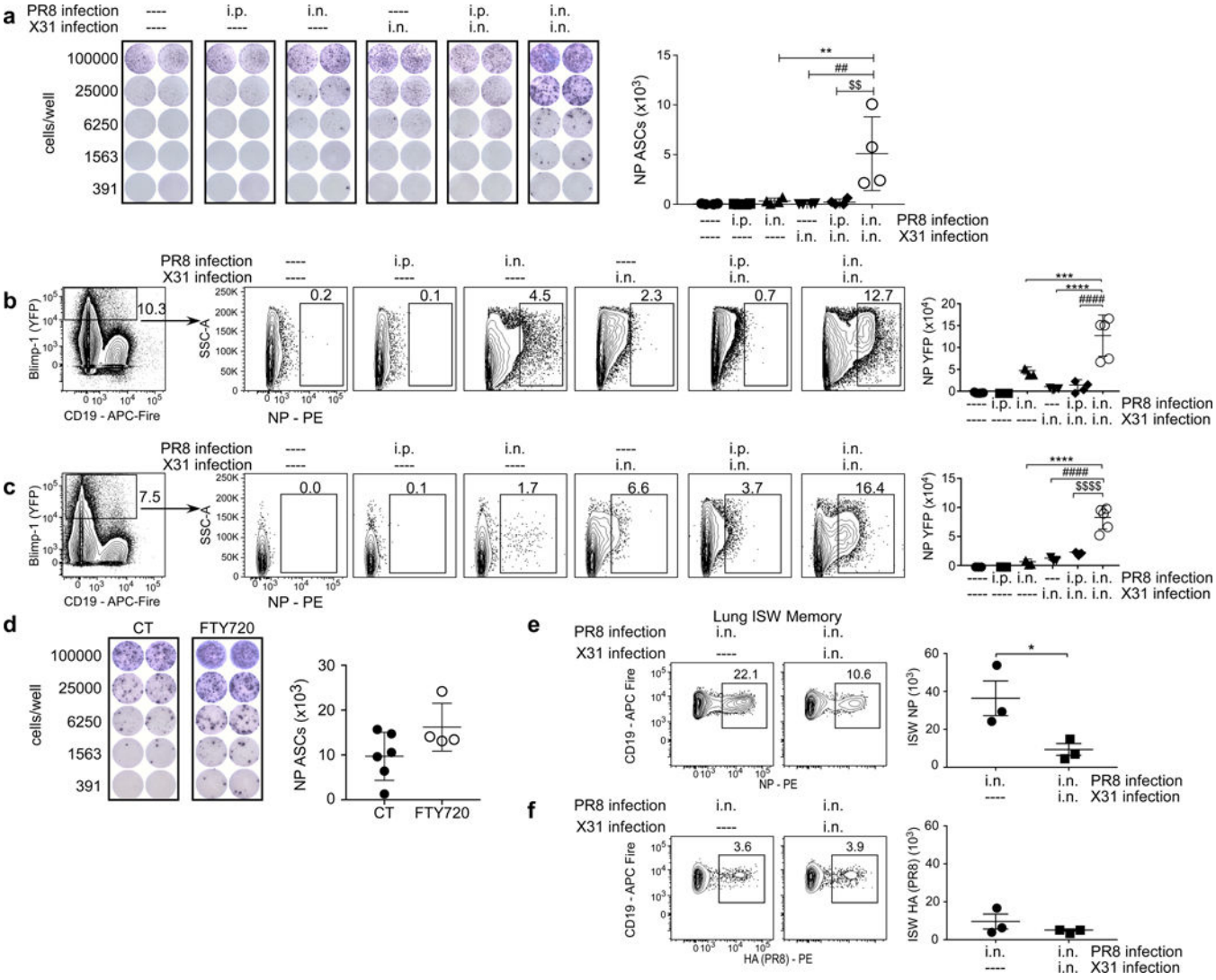

Fig. 8. BRM cells are required for rapid secondary ASCs in the lung.

a. NP–specific ELISPOTs in the lung 4 days after challenge infection. Graph shows data points as well as mean ± SD. Data are representative of 5 independent experiments with 4 mice/group. Data were analyzed with one–way ANOVA and Tukey's test for multiple comparisons, **p=0.0037, $^{\#\#}$p=0.002, $^{\$\$}$p=0.003. **b–c**. BLIMP–1–reporter mice were infected with PR8 on day 0, challenged with X31 on day 30 (**b**) or 60 (**c**) and ASCs were enumerated 3 days later. Cells in the lung were gated on live, singlet, lymphocytes (Supplementary Fig. 1a) and subsequently gated on NP–specific YFP^{+} cells. Data are representative of 3 independent experiments (**b**) or 2 experiments (**c**) with 3–5 mice/group. Graphs show individual data points as well as mean ± SD. Data are analyzed by 1–way ANOVA with Bonnferoni–Sidak test for multiple comparisons, ***p=0.0003, ****p=0.0001, $^{\#\#\#\#}$p=0.0001 (**b**) or Tukey's test for multiple comparisons, ****p=0.0001 $^{\#\#\#\#}$p=0.0001 $^{\$\$\$\$}$p=0.0001 (**c**). **d**. Mice were infected with PR8 on day 0, treated with FTY720, challenged with X31 on day 30 and ELISPOTs in the lung were analyzed 4 days later. Data are representative of 2 independent experiments with 6 mice/group (control) or 4

mice/group (FTY720). Graph shows data points as well as mean ± SD. Data were analyzed with a Mann–Whitney U test. **e–f**. Mice were infected with PR8 on day 0, challenged with X31 on day 30 and analyzed on day 33. Cells from the lung were gated on live, singlet, lymphocyte, $CD19^{+}B220^{-}CD38^{+}IgD^{-}IgM^{-}$ ISW memory B cells (Supplementary Fig. 1e) and NP–specific (**e**) HA(PR8)–specific (**f**) memory B cells were enumerated. Graphs show individual data points as well as mean ± SD. Data are representative of 3 independent experiments with 3 mice/group. Data were analyzed with Student's t test, *p=0.0488. $p<0.05$ is considered significant.